Nanoscale

Accepted Manuscript

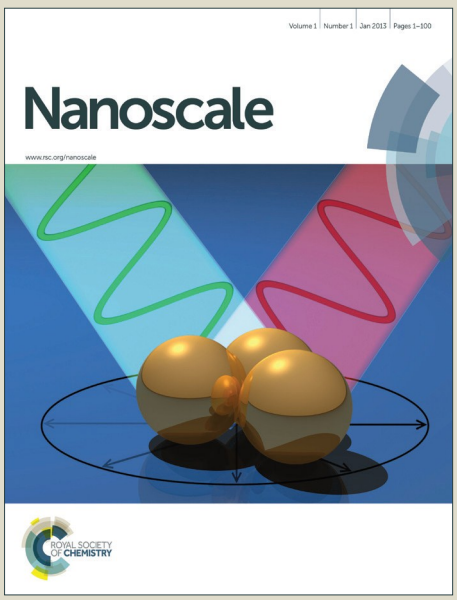

ROYAL SOCIETY OF CHEMISTRY

www.rsc.org/nanoscale

Nanoscale

ARTICLE

Thermodynamic Approach to Boron Nitride Nanotube Solubility and Dispersion

Received 00th January 20xx,
Accepted 00th January 20xx

DOI: 10.1039/x0xx00000x
www.rsc.org/

A. L. Tiano,[a] L.Gibbons, [a] M. Tsui,[b] S. I. Applin,[a] R. Silva,[c] C. Park[d] and C. C. Fay[d]

Abstract: Inadequate dispersion of nanomaterials is a critical issue that significantly limits the potential properties of nanocomposites and when overcome, will enable further enhancement of material properties. The most common methods used to improve dispersion include surface functionalization, surfactants, polymer wrapping, and sonication. Although these approaches have proven effective, they often achieve dispersion by altering the surface or structure of the nanomaterial and ultimately, their intrinsic properties. Co-solvents are commonly utilized in the polymer, paint, and art conservation industries to selectively dissolve materials. These co-solvents are utilized based on thermodynamic interaction parameters and are chosen so that the original materials are not affected. The same concept was applied to enhance the dispersion of boron nitride nanotubes (BNNTs) to facilitate the fabrication of BNNT nanocomposites. Of the solvents tested, dimethylacetamide (DMAc) exhibited the most stable, uniform dispersion of BNNTs, followed by N,N-dimethylformamide (DMF), acetone, and N-methyl-2-pyrrolidone (NMP). Utilizing the known Hansen solubility parameters of these solvents in comparison to the BNNT dispersion state, a region of good solubility was proposed. This solubility region was used to identify co-solvent systems that led to improved BNNT dispersion in poor solvents such as toluene, hexane, and ethanol. Incorporating the data from the co-solvent studies further refined the proposed solubility region. From this region, the Hansen solubility parameters for BNNTs are thought to lie at the midpoint of the solubility sphere: 16.8, 10.7, and 9.0 $MPa^{1/2}$ for δ_d, δ_p, and δ_h, respectively, with a calculated Hildebrand parameter of 21.8 $MPa^{1/2}$.

[a] *National Institute of Aerospace, 100 Exploration Way, Hampton, VA 23666, USA*
[b] *University of California, Berkeley, Berkeley, CA 94720, USA*
[c] *University of Texas at Brownsville, Brownsville, TX 78520, USA*
[d] *Advanced Materials and Processing Branch, NASA Langley Research Center, Hampton, VA 23681, USA*
† Corresponding author: cheol.park-1@nasa.gov

Electronic Supplementary Information (ESI) available: [details of any supplementary information available should be included here]. See DOI: 10.1039/x0xx00000x

Introduction

The boron nitride nanotube (BNNT) is a structural analogue of the carbon nanotube (CNT) and is composed of hexagonal B-N bonds.[1,2] The electronegativity difference between boron and nitrogen, results in partial ionic bonding.[3] Thus, BNNTs are electrically insulating with a fixed band gap,[1,4] while CNTs can be conductive or semiconducting. BNNTs also exhibit excellent mechanical properties,[5-7] better thermal stability than CNTs,[8] high thermal conductivity,[9] good chemical stability,[10] piezoelectric response,[11-13] and neutron radiation protection.[3,13-15] BNNTs have been produced from a variety of synthetic methods: combined ball-milling with subsequent annealing,[16] catalyst-based chemical vapor deposition (CVD),[17] arc-discharge,[2,18] laser vaporization,[19,20] plasma-enhanced pulsed laser deposition (PLD),[21] as well as the catalyst-free high temperature pressure (HTP) laser heating method.[22] Recently, significant progress has been made in increasing the yield of BNNTs through plasma-based syntheses: a hydrogen-catalyzed induction thermal plasma process[23] and a high-temperature, extended pressure inductively-coupled plasma method[24] capable of generating BNNTs at 20 g/h and 35 g/h, respectively. Additionally, the BNNTs have recently been made commercially available.

Many of the intrinsic properties of BNNTs are advantageous for nanocomposite fabrication. Dispersing nanotubes in a matrix can be problematic as a result of the various intermolecular forces between individual tubes, causing them to bundle and aggregate.[25-26] Methods to exfoliate bundles and disperse CNTs have already been extensively researched and examples include covalent surface functionalization, surfactants, polymer wrapping, and harsh treatment methods such as high power tip sonication with individual solvents.[27-29] However, most of these methods alter or damage the sp^2 nature of the nanotube surfaces which can weaken their properties before they are integrated into a composite. An ideal method would effectively disperse the tubes without modifying the nanotube surface, ensuring that the intrinsic properties originating from the sp^2 bonding would be preserved. In the case of BNNTs, limited studies on the dispersion and exfoliation have been reported using sonication as well as functionalization *via* polymers, surfactants, and other biomolecules.[30-36] This research utilizes a thermodynamic approach to determine the Hansen solubility parameters for BNNTs, and identifies good solvents and co-solvent systems for their dispersion. A brief discussion of solution thermodynamics and the graphical approach utilized herein are discussed below.

Solution Thermodynamics

Solution thermodynamics can be used to describe the mixing of multiple components via the Gibbs free energy of mixing (ΔG_{mix}) equation (Equation 1) where ΔH_{mix} is the enthalpy of mixing, T is the temperature in Kelvin, and ΔS_{mix} is the entropy of mixing.

$$\Delta G_{mix} = \Delta H_{mix} - T\Delta S_{mix} \qquad (1)$$

The components of a solution will spontaneously mix and create a homogenous solution if ΔG_{mix} is negative. Nanotubes have been shown to behave like long, rigid polymer chains, resulting in a small ΔS_{mix}.[37-39] Thus, to dissolve nanotubes successfully, a small or negative ΔH_{mix} is needed to minimize Gibbs free energy.

The Hansen solubility method, founded on the notion that "like dissolves like", is used to choose solvents for the solute that minimize the enthalpy of mixing.[40] Co-solvents, or a mixture of solvents, have the potential to enhance the solubility of a solute as compared to a single solvent[40,41] by better matching the Hansen solubility parameters of the co-solvent to the solute, thus minimizing ΔH_{mix}. This is commonly exploited in many other fields (such as polymer, paint, and art conservation) in order to selectively dissolve components without damaging materials with dissimilar solubility parameters. Moreover, toxic and costly solvents can be mimicked with a co-solvent mixture making this method potentially more cost effective and environmentally friendly. The solubility theory has been utilized to determine good solvents for dispersing single-walled carbon nanotubes (SWNTs).[42-45] Here, this approach is applied to develop good single solvents and co-solvents that improve the solubility of BNNTs with minimal sonication.

The Hansen solubility parameters for dispersion (δ_d), polar (δ_p), and hydrogen (δ_h) bonding, represent the intermolecular interactions contributing the solubility of a solute in a given solvent. Together the Hansen solubility parameters represent the Hildebrand parameter (δ_t), a numerical representation of the interaction between materials, as shown in Equation 2.[40]

$$\delta_t^2 = \delta_d^2 + \delta_p^2 + \delta_h^2 \qquad (2)$$

The Hildebrand solubility parameter (δ_t) of various solvents is often utilized to determine suitable solvents for a specific solute. Recently, Dadmun and co-workers explored the solubility of BNNTs in a few common solvents to determine a Hildebrand solubility parameter of 18.53 ± 1.07 $MPa^{1/2}$ for large diameter BNNTs (30 – 100 nm) with sonication.[36] However, Bergin *et al.* demonstrated for CNTs that the Hildebrand parameter lacks the specificity needed to identify solvents and is dependent on the nanotube diameter.[42] This suggests that the Hildebrand parameter (and by relation the Hansen solubility parameters) may not be an intrinsic value to express all possible interactions between materials and other factors, such as surface energies and entropic effects, should be considered when using solubility parameters. Bergin *et al.* suggested new parameters based on the surface energy, rather than the cohesive energy density, with dispersion, polar, and hydrogen bonding components being better for predicting nanotube-solvent interactions. Both methods remain imperfect, but Hansen solubility parameters are more practical and have been used successfully for nanomaterial dispersion.[42-45]

A graphical approach to Hansen solubility theory involves plotting the solvents and solutes in three-dimensional (3D) "Hansen space" with coordinates given by (δ_d, δ_p, δ_h) with the dispersion state or quality of the solute.[40] The solute point sits in the center of a solubility sphere with an experimentally determined radius (R_0). Any solvent inside the sphere is capable of dissolving the solute, with solvent strength increasing as one gets closer to the center of the sphere. The distance between the solvent and the solute can be calculated using Equation 3 to yield the value of R_a.

$$R_a^2 = 4(\delta_{d1} - \delta_{d2})^2 + (\delta_{p1} - \delta_{p2})^2 + (\delta_{h1} - \delta_{h2})^2 \qquad (3)$$

$$RED = R_a/R_0 \qquad (4)$$

Using the values of R_0 and R_a, the relative energy difference (RED) can be calculated to determine where the mixture is located in Hansen space (Equation 4).[40] An RED less than 1 is most favourable, indicating that the solvent is within the solubility sphere of the solute and dispersion will occur. If the RED equals 1, the mixture lies on the border of the solubility sphere of the solute. Thus the solute may only partially dissolve. If the RED is greater than 1, the solvent lies outside the solubility region of the solute and, thus the solute will not dissolve. As such, this methodology can be exploited to determine the solubility parameters for various nanomaterials by matching the solubility parameters of the solvents to approximate those of the nanostructured solute. Herein, this graphical approach was utilized to test the ability of single solvents to disperse BNNTs. N,N-dimethylacetamide (DMAc) exhibited the best dispersion of BNNTs (0.25 mg/mL) after 30 minutes of bath sonication, at that concentration, up to 1 month without any appreciable sedimentation of the nanotubes. This was followed by N,N-dimethylformamide (DMF), which displayed significant separation of the nanotubes after only 24 hours of settling. Similar observations were also noted for acetone and N-methyl-2-pyrrolidone (NMP), and to a lesser degree, isopropanol (IPA), methanol, and tetrahydrofuran (THF). The Hansen solubility parameters for BNNTs were approximated and applied Equation 2 to calculate the Hildebrand solubility parameter for BNNTs yielding values of δ_d = 16.8 $MPa^{1/2}$, δ_p = 10.7 $MPa^{1/2}$, δ_h = 9.0 $MPa^{1/2}$, and δ_t = 21.8 $MPa^{1/2}$.

Results and discussion

Single solvent studies

Figure 1 shows a representative transmission electron microscope (TEM) micrograph for raw BNNTs, with insets depicting a single-wall BNNT (SWBNNT), a double-wall BNNT (DWBNNT), and a three-wall BNNT (3WBNNT). The as grown BNNTs appear very thin and long with high aspect ratio, and shows flexible bundles of tubes with entangled tube aggregates.

First, in order to estimate a region of BNNT solubility in Hansen space, a variety of individual solvents were chosen with a wide range of solubility parameters. The full list of solvents is presented in Table 1 along with their corresponding Hansen and Hildebrand solubility parameters. Each solvent was mixed with raw BNNTs as-generated by the HTP method (Figures 1 and S1).[22] The dispersion state of each solvent after 1) stirring only (96 hrs), 2) stirring (96 hrs) and subsequent 30 minutes of sonicating the stirred sample and 3) after 1 week of settling time post sonication is also shown in Table 1. These results are discussed more in detail below. The dispersion state was classified into three categories: sedimented, swollen, or dispersed, based on the description provided previously by Ham *et al.*[46]

Images of all single solvent studies are shown in Figure S3 before stirring (Figures S3A, S3B), immediately after stirring (Figures S3C, S3D) and immediately after 30 minutes of sonication (Figures S3E, S3F). It was observed that many of the samples display very different dispersion states before and after the addition of sonication. Specifically, after only stirring, the solutions contained only swollen or sedimented BNNTs. After the addition of sonication, vials containing BNNTs in acetone, IPA, methanol, DMAc, DMF and THF exhibit turbid white solutions, which is indicative of dispersed BNNTs. Several other solvents, namely NMP, toluene, acetic acid, chloroform, and dichloromethane (DCM) displayed minor dispersion of BNNTs as some minor turbidity was observed immediately after sonication (Figures S3E, S3F). These observations are not surprising given that ultrasonic cavitation at high frequency has been shown to overcome the intermolecular forces between the nanotubes to open up gaps between the tubes, thereby separating the bundles into individual tubes.[48] Good solvents have a higher or comparable affinity to the individual tubes compared to the nanotube-nanotube affinity. Poor solvents have lower affinity, resulting in swollen BNNTs or sediment. As a result, the ΔG_{mix} of the dispersed state is comparable or lower than before sonication, and the individual nanotubes can be separated without aggregation. Based on the visual inspection immediately following sonication, the solvents were ranked qualitatively accordingly to their ability to effectively disperse BNNTs as follows: DMAc > DMF > THF > MeOH > IPA > acetone > chloroform ≈ DCM > NMP ≈ pyridine ≈ toluene ≈ DMSO ≈ acetic acid > ethanol > hexane >>> water.

The stability of the dispersions was also assessed after 1 day (Figures S3G, S3H) and 1 week (Figures S3I, S3J). In most cases, noticeable settling of BNNTs occurred after 24 hours as evinced by the decrease in the opaqueness for DMF, THF, MeOH, IPA, and acetone. Although some settling occurred in these cases, many BNNTs remained dispersed even after 24 hours of settling (Figures S3G, S3H) that indicates that a stable dispersion is maintained over this time period. Minor decreases in opacity were also observed for acetic acid, NMP, pyridine, chloroform, and DCM. Only DMAc maintained the dispersion of BNNTs after 24 hours post sonication. In the case of DMSO, the BNNTs were found to return to a sediment state after settling for 24 hours without any evidence of dispersion. Similarly, note that the BNNTs that were previously suspended/floating on the top of the solutions after sonication (IPA, MeOH, and acetic acid) settled after 24 hours and remained swollen in IPA and acetic acid. Interestingly, some raw BNNTs remain floating at the top of the acetic acid solution even after 24 hours of settling time, as was observed for water after stirring and sonication. Interestingly, some raw BNNTs remain floating at the top of the acetic acid solution even after 24 hours of settling time, as was observed for water after stirring and sonication.

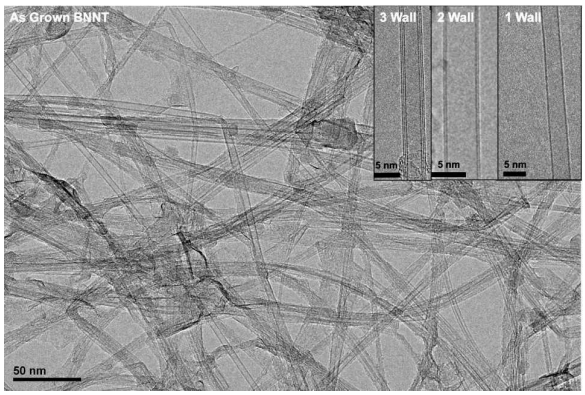

Figure 1. TEM micrograph of raw BNNTs showing single-wall (SWBNNT), double-walled (DWBNNT) and a BNNT with three walls (3WBNNT) in the insets.

Nanoscale

ARTICLE

Table 1. Dispersion state of BNNTs in various solvents after stirring, stirring with 30 minutes sonication, and after 1 week of settling time. The corresponding Hansen (δ_d, δ_p, δ_h) and Hildebrand (δ_t) solubility parameters, values for R_a and RED, and chemical structures are also given for each solvent.[47] Additional parameters for solvents such as density and surface tension can be found in Table S1.

Solvent	δ_d, MPa$^{1/2}$	δ_p, MPa$^{1/2}$	δ_h, MPa$^{1/2}$	δ_t, MPa$^{1/2}$	Structure	Dispersion state (stirring only)	Dispersion state (stirring + 30 mins sonication)	Dispersion state (after 1 week settling time)	R_a [e]	RED [f]
N,N'-dimethylacetamide (DMAc)	16.8	11.5	10.2	22.5	$CH_3C(O)N(CH_3)_2$	sediment	dispersed	dispersed	1.44	0.34
N,N'-dimethylformamide (DMF)	17.4	13.7	11.3	24.9	$HC(O)N(CH_3)_2$	swollen	dispersed/swollen	dispersed/swollen	3.97	0.92
acetone	15.5	10.4	7.0	19.9	CH_3COCH_3	sediment	dispersed/swollen	dispersed/swollen	3.29	0.77
methanol	15.1	12.3	22.3	29.6	CH_3OH	swollen	dispersed/swollen [b]	swollen	13.82	3.21
isopropyl alcohol (IPA)	15.8	6.1	16.4	23.6	$(CH_3)_2CHOH$	swollen	dispersed/swollen [b]	sediment	8.94	2.08
tetrahydrofuran (THF)	16.8	5.7	8.0	19.4	$(CH_2)_4O$, cyclo	swollen	dispersed/swollen	swollen	5.10	1.19
N-methyl-2-pyrrolidone (NMP)	18.0	12.3	7.2	23.0	$HN((CH_2)_3CO)$, cyclo	swollen	dispersed/swollen [a]	dispersed/swollen	3.40	0.79
chloroform	17.8	3.1	5.7	19.0	$CHCl_3$	sediment	swollen [a]	swollen	8.52	1.98
dichloromethane	18.2	6.3	6.1	20.0	CH_2Cl_2	swollen	swollen [a]	swollen	5.97	1.39
acetic acid	14.5	8.0	13.5	21.4	CH_3COOH	swollen [*]	swollen [a,b,d]	swollen	6.98	1.62
dimethylsulfoxide (DMSO)	18.4	16.4	10.2	26.7	$(CH_3)_2SO$	swollen	swollen	swollen	6.65	1.55
toluene	18.0	1.4	2.0	18.2	$C_6H_5CH_3$, cyclo	sediment	swollen [a]	swollen	11.88	2.76
pyridine	19.0	8.8	5.9	21.8	C_5H_5N, cyclo	sediment	sediment [c]	sediment	5.71	1.33
ethanol	15.8	8.8	19.4	26.5	C_2H_5OH	swollen	sediment	sediment	10.76	2.50
hexane	15.3	0.0	0.0	15.3	$CH_3(CH_2)_4CH_3$	sediment [a]	sediment	sediment	14.30	3.33
water	15.6	16.0	42.3	47.8	H_2O	n/a [d]	n/a [d]	n/a [d]	33.80	7.86

[a] Minor turbidity was observed indicating a small amount of BNNTs were dispersed.
[b] BNNTs were suspended at the top of the solution immediately following sonication.
[c] BNNTs were broken up but adhered to the walls of the sample vial.
[d] Some raw BNNT pieces remaining on top of vial. In water, all raw BNNTs were unaffected by the processing methods; pieces remained on top of the solution.
[e] Calculated using 16.8, 10.7, and 9.0 MPa$^{1/2}$ for δ_d, δ_p, and δ_h, respectively for BNNT.
[f] Calculated using R_0 = 4.3 MPa$^{1/2}$ by expanding the boundary to ensure the poor solvents appear outside the sphere.

This is a further indication that acetic acid is a poor solvent for BNNT dispersion. For IPA, MeOH, and acetic acid, it is plausible that a combination of cavitation and capillary (surface tension) forces are responsible for the short-term buoyancy of BNNTs in these solvents. Under sonication at 45 kHz, cavitation generates a bubble at the interface between the solvent and nanotubes, or trapped inside the bundles between the nanotubes, could cause them to float on top of the solution. In the event that voids form, they can be wetted *via* capillary action over time, causing the bundles to settle. The settling time will be affected by the density and viscosity of the solvent (see Table S1) according to Stokes' law. Note that this

may also influence the stability test as a function of time and corresponding UV-Vis results.

After 1 week of settling (Figures S3I, S3J), additional sedimentation of BNNTs occurred in all cases, except DMAc, where no change in the dispersion state was observed. This indicates that BNNT dispersion in DMAc is very stable and uniform, even at a high concentration of 0.25 mg/mL. This sample was analyzed with SEM to determine the state of the nanotubes after sonication (Figure 2). At lower magnification (Figure 2A), it was observed that much of the lacey carbon film was covered with long, thin, flexible nanotubes, which looked similar to the raw BNNTs before sonication shown in Figure S1. No shortened nanotubes were found in the micrographs taken after sonication. At higher resolution (Figure 2B), the BNNTs appeared to be intact and maintain their length. In addition, no noticeable peaks other than B-N modes showed up in FTIR spectra after sonication (Figure S4), demonstrating that the 30 minutes of sonication did not noticeably damage the nanotube structure.

DMF also maintained a fairly opaque solution on top after 1 week, which implies that BNNT dispersion in DMF is relatively stable, but presumably at a lower concentration than 0.25 mg/mL. Additionally, acetone and NMP solutions maintain some dispersed

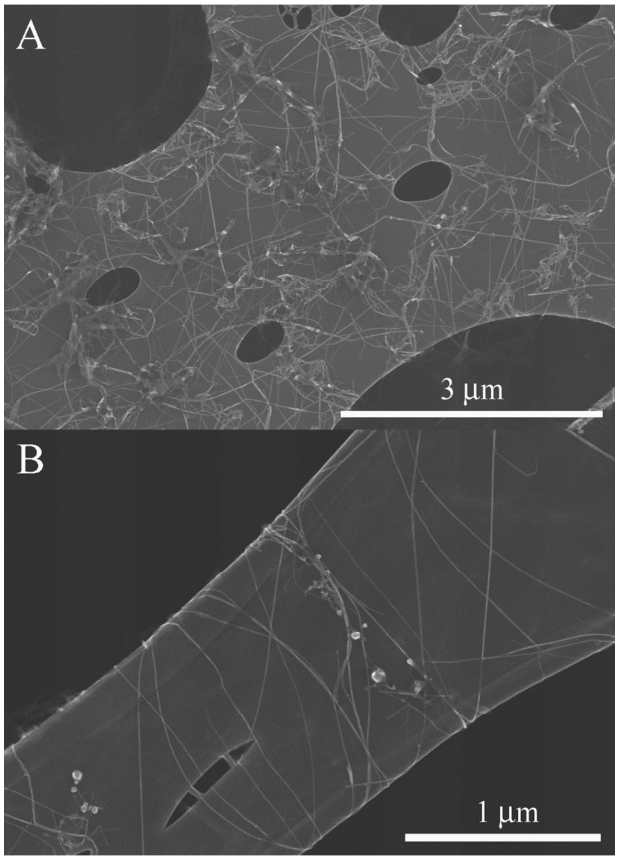

Figure 2. Representative SEM images of BNNTs dispersed in DMAc after mild sonication showing a large area covered with nanotubes (A) and a magnified area showing the nanotube structure is intact after sonication (B).

BNNTs even after one week as evidenced by the slight turbid appearance of the supernatant. By contrast, THF, IPA, and MeOH all exhibited significant sedimentation of the BNNTs after 1 week, suggesting the dispersion achieved in these solvents after sonication is not stable. The BNNTs did remain swollen in both THF and IPA following sedimentation of the dispersed solution, which suggests there is some affinity between the BNNTs and these solvents. Based on these observations, DMAc, DMF, acetone and NMP were determined as excellent solvents for stable, long term dispersion of BNNTs while THF, IPA and MeOH are suitable for metastable, short-term (<24 hours) dispersion.

The chemical and physical properties of the solvents can also be utilized to understand why certain solvents are more effective in dispersing BNNTs. When comparing the solvents, differences in the chemical and physical properties may explain the observed results. For example, the best solvents DMAc and DMF both contain nitrogen and are Lewis bases. Hence, chemical composition of the solvents and, potentially, Lewis acid/base chemistry could play a role in dispersion. Lewis bases (amines and phosphines) have been employed successfully for the functionalization of bamboo-like BNNTs, which act as a Lewis acid, to achieve stable dispersion in solvents like toluene, benzene, and tributylamine.[50] The solvents DMAc, DMF, DMSO, NMP, THF, acetone, and pyridine are all Lewis bases. Of these solvents, pyridine and DMSO are stronger Lewis bases than DMAc and DMF. If Lewis acid/base chemistry was the only key factor in dispersion, then all of these solvents would produce stable dispersion of BNNTs, but this is not the case. DMAc displayed the best dispersion stability (higher affinity) for individual BNNTs. Similarly, for NMP, the dispersed BNNTs also remained stable over time, although the amount of BNNTs dispersed was much lower than in DMAc. For DMF, DMSO, THF, and acetone, significant settling was observed over time following the sonication, indicating that BNNTs are less stable (lower affinity) in these solvents. In the case of DMSO, which contained only swollen BNNTs, all of the BNNTs form a sediment after only 24 hours.

While it is evident that many Lewis bases are excellent solvents for BNNTs, the selection of suitable solvent cannot solely rely on Lewis acid-base interactions. Upon further examination it is apparent that there may be competing effects from the surface tension of the various solvents (Table S1). For example, DMSO has a higher surface tension (42.9 mJ/m^2) as compared to DMAc (32.4 mJ/m^2) in addition to a larger value for δ_p. Similarly, pyridine also has a higher surface tension (36.7 mJ/m^2) and a smaller value for δ_p as compared to DMAc. By comparison, NMP also has a high surface tension (44.6 mJ/m^2) but its polar component (12.3 $MPa^{1/2}$) is very close to that of DMAc (11.5 $MPa^{1/2}$). Yum and Yu experimentally determined the surface tension for individual BNNTs using the Wilhelmy method to be 26.7 mN/m.[49] These results suggest that it may be difficult to wet the surface of BNNTs for solvents with higher surface tension that also possess less than ideal polar components. This reinforces that there are many effects and parameters to consider when attempting to disperse nanomaterials. A single approach which encompasses all of these effects remains to be developed. Since the intermolecular forces from composition and structural effects are encompassed in solubility theory, the Hansen solubility parameters provide a practical and reliable approach to understanding the solubility of nanomaterials.

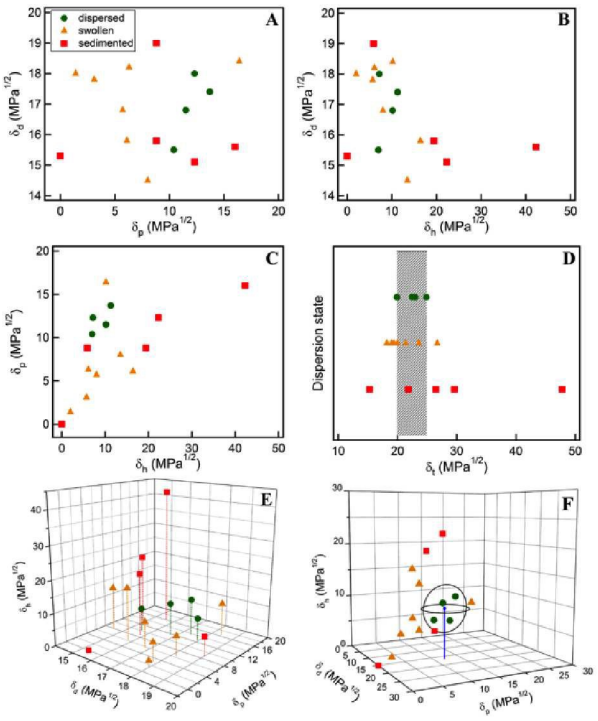

Figure 3. 2D plots of the Hansen solubility parameters for individual solvents versus the dispersion state immediately following sonication: (A) dispersion component (δ_d) versus polar component (δ_p), (B) dispersion component (δ_d) versus hydrogen bonding component (δ_h), and (C) polar component (δ_p) versus hydrogen bonding component (δ_h) along with a plot of the dispersion state versus the Hildebrand solubility parameter (δ_t) (D), a 3D plot of all three parameters (E), and a plausible solubility sphere for BNNTs (F). The shaded region in (D) corresponds to the range for δ_t determined from the dispersed single solvent studies. Note that the point for water is not present in (F) as a result of the scale of the axes. The symbols ■, ▲, and ● refer to the sedimented, swollen, and dispersed states, respectively.

The solubility parameters of each single solvent can subsequently be utilized to define a broad region of BNNT solubility in 3D Hansen space. Of these solvents that worked well, DMAc dispersed the as-produced BNNT material best, followed by DMF, acetone, NMP, and IPA ≈ THF ≈ MeOH. DMAc, DMF, acetone, and NMP exhibited long-term stability, while the latter solvents are better suited for short-term dispersion of BNNTs. Thus, the solubility region of BNNT should be near the solubility parameters of these solvents and may be centered about DMAc with IPA, MeOH and THF just outside (or on the border) of the solubility sphere. These solvents define range for δ_d, δ_p, and δ_h as 15.1 – 18.0, 10.4 – 13.7, and 7.0 – 11.3 $MPa^{1/2}$, respectively. The mid-point of the range of each parameter is 16.8, 12.1, and 9.2 $MPa^{1/2}$, which, not surprisingly, closely matches those of DMAc (16.8, 11.5, and 10.2 $MPa^{1/2}$).

In order to fully understand the dispersion of BNNTs, it is desirable for the individual Hansen solubility parameters to be explored. Figure 3 provides 2D plots of the Hansen solubility parameters (Figures 3A–C) and the Hildebrand parameter (Figure 3D) versus the long-term dispersion state for all the single solvents tested, as well as a 3D plot without (Figure 3E) and with a plausible solubility region (sphere) depicted (Figure 3F).

The 2D plots in Figures 3A–C help to shed some additional light on the solubility region of BNNTs. In Figure 3A, the best solvents are clearly grouped together. While the good solvents are distributed across a large range for the dispersion component (δ_d), the polar component (δ_p) evinces a clear region of solubility. The large range for δ_d can also be observed in Figure 3B, while the good solvents occupy a narrow range of the hydrogen bonding component (δ_h). These observations suggest that the dispersion component may be the least significant of the Hansen solubility parameters. By contrast, both the polar (δ_p) and hydrogen bonding (δ_h) components appear to be critical for achieving dispersion of BNNTs.

In Figure 3C, the best solvents are closely grouped together in a narrow region of δ_p and δ_h, which is apparent in the 3D plot (Figure 3E). This suggests that both the polar and hydrogen bonding components need to be within this region in order to be a suitable solvent for BNNTs. For example, DMSO is a strong Lewis base which was anticipated would interact well with BNNTs, however no turbid solution was observed even after sonication. DMSO has a hydrogen bonding component (δ_h) of 10.2 $MPa^{1/2}$, identical to DMAc, which should belong to the dispersed category, but a swollen state is maintained after sonication and forms a sediment over time. In this case, the dispersion state may be affected by DMSO's high polar component (δ_p) of 16.4 $MPa^{1/2}$, which is close to that of water (16.0 $MPa^{1/2}$), and lies outside the estimated range for δ_p (10.4 – 13.7 $MPa^{1/2}$). As mentioned previously, the behavior of BNNTs in DMSO as a result of its high surface tension and relatively high viscosity (1.99 cP) cannot be discounted as this may impede wetting of the BNNT surface and/or the cavitation effect under sonication. Similar observations hold true for methanol, which displayed a high degree of dispersed BNNTs after sonication, though it has a very high δ_h value of 22.3 $MPa^{1/2}$. However, its polar component (δ_p = 12.3 $MPa^{1/2}$) is between that of DMAc and DMF, which may result in the temporary dispersion of BNNTs. The effects of the hydrogen bonding component shows drastic results at the extremes as demonstrated by water (δ_h = 42.3 $MPa^{1/2}$) and hexane (δ_h = 0.0 $MPa^{1/2}$). In water, even after stirring and sonication, the raw BNNT pieces remained completely intact. Conversely, while in hexane, the BNNTs behaved as though they were repelled by the solvent and adhered to the walls of the sample vial. As shown in a plot of dispersion state versus δ_t (Figure 3D), several solvents lie within the range of the selected best solvents, 19.9 – 24.9 $MPa^{1/2}$, but do not effectively disperse the nanotubes (*i.e.* pyridine, acetic acid, dichloromethane). It is evident from these ranges that the dispersion state cannot be solely explained by the Hildebrand solubility parameter (δ_t). Overall, these observations are consistent with Ham *et al.*,[46] reinforcing that the individual Hansen solubility parameters can adequately describe the interaction between BNNTs and solvents over the Hildebrand solubility parameter. Since DMAc displayed the most uniform, stable dispersion, the solubility parameters for BNNT may closely resemble those of DMAc.

Based on these observations, the calculated midpoints (16.8, 12.1, and 9.2 $MPa^{1/2}$) determined from the single solvent studies are postulated to be the solubility parameters for BNNTs. To test this scenario, a solubility sphere was generated in 3D Hansen space about this point (Figure 3F). The final radius of 4.3 $MPa^{1/2}$ was determined by expanding the boundary to ensure the poor solvents appear outside the region. Indeed, all of the good solvents (DMAc,

DMF, acetone, and NMP) are encompassed within the proposed solubility region. This proposed solubility region is in good agreement with the visual observations for BNNT dispersion as well as the values of R_a for the solvents (Table 1). The experimentally determined values of δ_d, δ_p, and δ_h for BNNTs were inserted into Equation 2 to calculate the Hildebrand parameter (δ_t). This results in δ_t = 22.6 $MPa^{1/2}$, which, like the Hansen solubility parameters, closely match the δ_t for DMAc (22.5 $MPa^{1/2}$). The difference in the experimentally determined Hildebrand parameter (δ_t) between the as-produced BNNT material studied here ($\delta_t \approx$ 22.6 $MPa^{1/2}$) and the study conducted by Mutz and co-workers (δ_t = 18.5 $MPa^{1/2}$)[36] indicate that the solubility parameters are sensitive to the nature of the tubes employed. Different experimental methods are expected to produce BNNTs with different inherent chemical and physical properties. Hence, this difference in Hildebrand parameters is not surprising given that the BNNTs utilized in each work varied in diameter, length, and so on. More importantly, our approach utilized Hansen solubility parameters from which the Hildebrand parameter was calculated, while Dadmun and co-workers focused solely on the Hildebrand parameter, which is not specific enough to select suitable solvents.[42] It is important to note that it may be necessary to repeat these studies for BNNTs fabricated with alternative techniques, production conditions, or purification methods. Based on the excellent agreement of the proposed solubility region with the visual observations for BNNT dispersion, it is likely that suitable solvents for dispersing BNNTs can be selected from within this region.

Co-solvent studies

Next, co-solvent mixtures were chosen from these single solvents to demonstrate the effectiveness of the experimentally determined solubility region. By utilizing co-solvents, the solubility parameters of the system can be tailored towards the desired region of BNNT solubility in 3D Hansen space. Hence, stable dispersions of BNNTs can be made, even with poor solvents. The chosen co-solvent systems are listed in Table 2 with their calculated solubility parameters and corresponding dispersion states. NMP, toluene, ethanol, hexane, DCM, DMSO, and water were categorized as poor solvents for this study. Each poor solvent was mixed with a miscible solvent that is relatively good for dispersing BNNT. Specifically, explored were co-solvent systems of IPA-DMF, DMF-DCM, THF-hexane, DMF-toluene, DMAc-water, DMAc-NMP, EtOH-acetone, DMF-acetone, THF-NMP, and DMSO-THF at 1:1 volume ratios of the solvents.

BNNTs were added to the co-solvent mixtures for a concentration of 0.25 mg/mL in an identical fashion as the single solvents. The resultant images are shown in Figure S5 before stirring (Figures S5A, S5B), immediately after stirring for 4 days (Figures S5C, S5D), immediately after 30 minutes sonication (Figures S5E, S5F), after 24 hours (Figures S5G, S5H) and 1 week of settling time (Figures S5I, S5J). Similar to the single solvent studies, almost all of the samples displayed dispersed or swollen BNNTs after stirring only with minor turbidity (Figures S5C, S5D). Of these co-solvents, DMF-acetone displayed the most dispersed BNNTs without sonication. For pure acetone and DMF alone, only sediment and swollen BNNTs were observed, respectively. This provides some evidence of the synergistic effects of a co-solvent on dispersing BNNT. Also note that the DMAc-water co-solvent displays swollen/sediment BNNTs. This is in contrast with the results obtained for pure water, which was incapable of breaking down the pieces of raw BNNTs even after subsequent sonication. This holds promise for aqueous-based dispersion of BNNTs without surfactants.

After 30 minutes of mild sonication, significantly different results were obtained (Figures S5E, S5F). All of the co-solvent samples, except for DMAc-water, display turbid dispersions of BNNTs. Only in the case of DMF-toluene was complete dispersion achieved; the remaining samples display a combination of dispersed BNNTs with some suspended (swollen) nanotubes. In the case of DMAc-water, the BNNTs were found to form a sediment after sonication. In this case, the nanotubes may quickly bundle during the exfoliation as a result of their hydrophobic nature. Hence, for NMP, toluene, ethanol, hexane, DCM, and DMSO, which are poor stand-alone solvents, BNNT dispersion was significantly improved by their combination with a suitable co-solvent. In addition, some of the co-solvent shows better dispersability for BNNTs compared to each single solvent after one week settlement (*e.g.* THF-NMP, DMSO-THF).

After settling for 24 hours (Figures S5G, S5H), all of the suspended/floating BNNTs were found to settle to the bottom of the sample vial. Some minor changes in the turbidity of the solution were also observed for DMF-DCM and EtOH-acetone. Following a full week of settling time (Figures S5I, S5J), additional sedimentation of BNNTs was clearly evinced for IPA-DMF, DMF-DCM, and slightly for DMF-toluene. Though the remaining co-solvent solutions all possess some swollen BNNTs, the majority of the turbid dispersions did not exhibit any significant changes after a week. Only the IPA-DMF and DMF-DCM dispersions displayed additional settling over time. These results demonstrate that the BNNT dispersions are highly stable and uniform in co-solvents of DMF-toluene, DMF-acetone, THF-NMP, DMSO-THF, DMAc-NMP, and THF-hexane.

By comparing visual observations after 1 week, it is expected that DMAc would be the best long-term solvent for BNNT dispersion. For a more quantitative comparison, the quality of all dispersions were analyzed with UV-Vis spectroscopy after 2 months of settling time to assess the long-term stability of BNNTs all of the tested solvents. The spectra for supernatants of all single solvents and co-solvent samples are displayed in Figures S6A and S6B, respectively. An absorbance point at 500 nm was used to compare the absorbance of each sample relative to each other. Based on these results, the individual solvents (Figure S6A) can be ranked as: DMAc > acetone > DMF = NMP > toluene > rest in terms of their long-term stability. Although both THF and IPA were found to be suitable solvents for BNNTs up to 24 hours post sonication (Figures S3G, S3H), the UV-Vis data provide further evidence that they are poor solvents for long-term dispersion of BNNTs. For the co-solvents (Figure S6B), the samples were ranked as: THF-NMP > DMF-acetone > DMSO-THF > DMAc-NMP ≈ THF-hexane ≈ DMF-toluene > EtOH-acetone ≈ IPA-DMF ≈ DMAc-H_2O ≈ DMF-DCM. These results are reasonably consistent with the visual observations after 1 week of settling time. Note that both THF-NMP (Abs = 0.63) and DMF-acetone (Abs = 0.40) displayed a higher absorbance value than DMAc alone (Abs = 0.33), which suggests that both of these co-solvents might be superior at maintaining a larger quantity of dispersed BNNTs over a long period of time.

Table 2. Dispersion state of BNNTs in co-solvent systems at a 1:1 ratio after stirring and after stirring and 30 minutes of sonication along with their calculated Hansen and Hildebrand solubility parameters, and values for R_a and RED.

Co-solvent	δ_d, MPa$^{1/2}$	δ_p, MPa$^{1/2}$	δ_h, MPa$^{1/2}$	δ_t, MPa$^{1/2}$	Dispersion state (stirring only)	Dispersion state (stirring + 30 mins sonication)	R_a[c]	RED[d]
THF-NMP	17.4	9.0	7.6	21.0	swollen	dispersed/swollen[b]	2.51	0.58
DMF-acetone	16.5	12.1	9.2	22.4	swollen[a]	dispersed/swollen[b]	1.54	0.36
DMAc-NMP	17.4	11.9	8.7	22.8	swollen[a]	dispersed/swollen	1.72	0.40
DMSO-THF	17.6	11.1	9.1	23.1	swollen	dispersed/swollen[b]	1.65	0.38
DMF-toluene	17.7	7.6	6.7	21.6	swollen	dispersed	4.26	0.99
IPA-DMF	16.6	9.9	13.9	24.3	sediment	dispersed/swollen[b]	4.98	1.16
ethanol-acetone	15.7	9.6	13.2	23.2	swollen	dispersed/swollen[b]	4.87	1.13
DMF-DCM	17.8	10.0	8.7	22.5	swollen	dispersed/swollen[b]	2.14	0.50
THF-hexane	16.1	2.9	4.0	17.4	sediment	dispersed/swollen	9.37	2.18
DMAc-water	16.2	13.8	26.3	35.2	swollen	sediment	17.62	4.10

[a]Minor turbidity was observed indicating a small amount of BNNTs were dispersed.
[b]Swollen BNNT were suspended at the top of the solution immediately following sonication.
[c]Calculated using 16.8, 10.7, and 9.0 MPa$^{1/2}$ for δ_d, δ_p, and δ_h, respectively for BNNT.
[d]Calculated using R_0 = 4.3 MPa$^{1/2}$.

However, comparing visual observations of these three samples after 1 week, the DMAc was expected to maintain a higher absorbance since the co-solvents had larger amounts of BNNT sediment. Comparing images after 1 month of settling time (Figure S7), the dispersion state of DMF-acetone and DMAc are nearly identical, while THF-NMP displays slightly less dispersed BNNTs. It is possible that the two co-solvent systems may contain more individual nanotubes or the co-solvents generate more thermodynamically stable dispersions of BNNTs than DMAc alone. Regardless, this provides further evidence that co-solvents have a synergistic effect that greatly promotes BNNT dispersion. Thus, the effectiveness of combining solvents to create a more stable dispersion of BNNTs than those generated in the individual solvents alone has been demonstrated.

All of these results present clear evidence that co-solvent combinations improve BNNT dispersion in otherwise poor solvents by improving their effective solubility parameters. Indeed, the majority of the suitable co-solvents have solubility parameters within (or on the border of) the ranges determined above (Table 2). The data for the co-solvents systems were also included in the 2D and 3D Hansen space plots (Figure 4) as a function of their long term dispersion state. These graphs provide visual reinforcement that many of the co-solvents lie within the experimentally proposed solubility region for BNNTs, as there are clear groupings of good single solvents (solid green circle) and co-solvents (solid green diamond) in Figures 4A, 4B, and 4C. This can also be observed in the 3D plot of all samples (Figure 4E). Figure 4D shows a plot of the dispersion state with respect to the Hildebrand parameter (δ_t) to further reinforce that choosing solvents based on δ_t alone is not a viable method.

From these graphs in Figure 4, some outliers are also clearly prevalent, specifically THF-hexane and DMF-DCM. DMF-DCM maintains parameters very close to the region proposed in Figure 3F (17.8, 10.0, and 8.7 MPa$^{1/2}$), but BNNTs are clearly separated as shown in the visual observations after 1 week (Figure S5I) and 1 month (Figure S7C). The UV-Vis data (Figure S6B) are in excellent agreement with the visual observations showing no absorbance over the range. Hence, DMF-DCM is a poor co-solvent system for BNNTs although it is within the proposed range. This may be a combination of poor affinity and density mismatch effects, since DCM has the second highest density (1.326 g/cm^3) of the solvents in this study, second only to chloroform (1.479 g/cm^3) while DMF has a density of 0.945 g/cm^3. Indeed, BNNTs demonstrated low affinity to both DCM and chloroform (Figure S3). Interestingly, in the case of THF-hexane, only the dispersion component (δ_d) is within the experimentally determined solubility region, but some BNNTs were unexpectedly dispersed after 1 week (Figure S5I). This distinctly contrasts the observations for pure hexane, in which BNNTs were repelled by the solvent. This indicates that even mild improvement towards this region of BNNT solubility still has a substantial effect on the dispersion of the nanotubes. It is plausible that introducing polar and hydrogen bonding behavior by adding THF to hexane (δ_p = δ_h = 0.0 MPa$^{1/2}$) increased BNNT dispersability. This was further explored by generating a 85:15 of THF:hexane to further increase

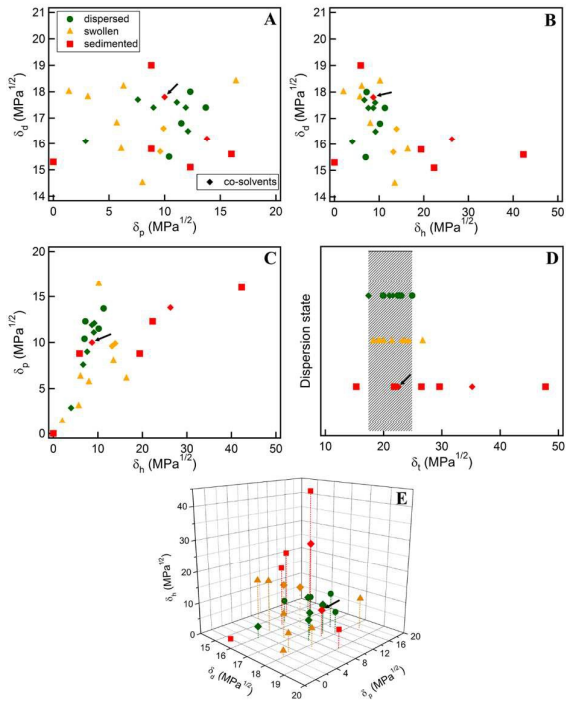

Figure 4. 2D plots of the Hansen solubility parameters for individual solvents and co-solvents versus the dispersion state: (A) dispersion component (δ_d) versus polar component (δ_p), (B) dispersion component (δ_d) versus hydrogen bonding component (δ_h), and (C) polar component (δ_p) versus hydrogen bonding component (δ_h) along with a plot of the dispersion state versus the Hildebrand solubility parameter (δ_t) (D), and a 3D plot of all three parameters (E). The shaded region in (D) corresponds to the range for δ_t determined from the dispersed single solvents and co-solvents studies. The symbols ■, ▲, and ● refer to the sedimented, swollen, and dispersed states of the single solvents, respectively. The symbols ♦, ♦, and ♦ refer to the sedimented, swollen, and dispersed states of the co-solvents, respectively. The small black arrow in each panel indicates the DMF-DCM outlier.

the polar and hydrogen bonding components towards the solubility region. This mixture has dispersion, polar, and hydrogen bonding components of 16.6, 4.8, and 6.8 MPa$^{1/2}$, respectively. A larger degree of white opaqueness was observed for this sample immediately after sonication (Figure S8A, left) and up to 1 week of settling time (Figure S8B, left). This reinforces that improvement towards the solubility parameters of the solubility region can greatly enhance the dispersion of BNNTs.

In the case of DMAc-water, both the dispersion and polar components are within the acceptable range. However, no turbid dispersion was observed and sedimentation occurs immediately after sonication. This can be attributed to the very large hydrogen bonding component (δ_h = 26.3 MPa$^{1/2}$) which has an adverse effect because of the hydrophobicity of BNNTs. This also contributes to an overall large Hildebrand solubility parameter (δ_t) of 35.2 MPa$^{1/2}$. In this case, the inclusion of the best single solvent cannot overcome the large hydrogen bonding component at a 50:50 ratio. In an effort to lower the hydrogen bonding component closer to that of DMAc, BNNTs were tested in a 90:10 ratio of DMAc:water with dispersion, polar and hydrogen bonding components of 16.7, 11.9, and 13.4

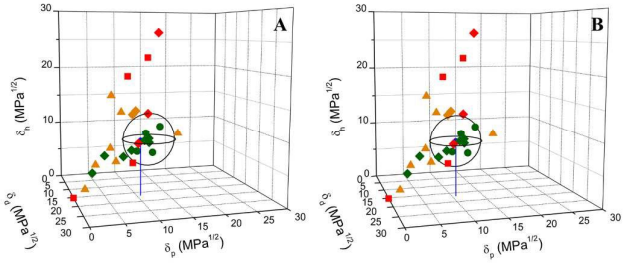

Figure 5. 3D Hansen space plots for all solvents and co-solvents tested with the solubility region predicted from the single solvent studies only (A) and with the co-solvent studies (B). The symbols ■, ▲, and ● refer to the sedimented, swollen, and dispersed states of the single solvents, respectively. The symbols ♦, ♦, and ♦ refer to the sedimented, swollen, and dispersed states of the co-solvents, respectively.

MPa$^{1/2}$. After sonication, some minor turbidity was observed (Figure S4A, right), which was slightly improved from the 50:50 mixture. After 1 week of settling time, only a swollen dispersion state was observed (Figure S8B, right). Although the dispersion may be short-lived, these additional studies for THF:hexane and DMAc:water demonstrate that by adjusting the ratios of the co-solvents, BNNTs can be dispersed in mixtures containing poor solvents (hexane and water).

Next, the proposed solubility region in Figure 3F was evaluated by including the co-solvent studies, including the additional THF:hexane (85:15) and DMAc:water (90:10) mixtures (Figure 5A). The solubility sphere (R_0 = 4.3 MPa$^{1/2}$) covers most of the good solvents and is centered about (16.8, 12.1, 9.2 MPa$^{1/2}$). This closely matches the solubility parameters for DMF-acetone (16.5, 12.1, and 9.2 MPa$^{1/2}$) which was determined to be a better solvent than DMAc alone from the UV-Vis data. Of the good co-solvents, only DMF:toluene and both THF:hexane (50:50 and 85:15) mixtures lie outside of this solubility region. Both THF:hexane mixtures are considered outliers with respect to their Hansen solubility parameters, so their inclusion is not expected, regardless of the solubility sphere chosen. On the other hand, it was expected that DMF:toluene would be incorporated as it lies closer to the other good solvents and co-solvents. As discussed previously, DMF:DCM is an outlier as a poor solvent near the middle of the region, likely due to density mismatch effects. The poor co-solvent of DMAc:water (90:10 mixture) is on the border of the solubility region, which is undesirable given the very poor affinity of BNNTs to the solvent (Figure S8).

Incorporating the solubility parameter values for the good co-solvents to the good single solvents (excluding THF:hexane), the midpoint is estimated to be 16.8, 10.7, and 9.0 MPa$^{1/2}$. A second solubility sphere was drawn about this point with the same radius as in Figure 5A (R_0 = 4.3 MPa$^{1/2}$) to yield the 3D sphere region shown in Figure 5B. In this region, all of the good co-solvents have been incorporated or lie on the edges of the region with the exception of the THF:hexane mixtures. In addition, the region is shifted down in the δ_h direction (z-axis), resulting in the 90:10 mixture of DMAc:water to correctly fall outside the region. If both regions are considered (excluding the DMF:DCM outlier), the second region (Figure 5B) is more plausible due to the incorporation of the best solvents and co-solvents. . This is in good agreement with the R_a and RED values calculated for all solvents (Table 1) and

co-solvents (Table 2). Based on this assessment, the Hansen solubility parameters for BNNTs are proposed to closely match the values of 16.8, 10.7, and 9.0 $MPa^{1/2}$ for δ_d, δ_p, and δ_h, respectively, with a calculated value of 21.8 $MPa^{1/2}$ for δ_t.

Experimental

Materials

The BNNTs were generated using the catalyst-free high temperature pressure (HTP) method reported earlier and the material is used as-synthesized, without any purification or modification.[22] Solvents utilized in this work were isopropyl alcohol (IPA, Chemsolv), methanol (MeOH, Fisher Scientific, Karl Fischer grade, anhydrous), toluene (Sigma-Aldrich, anhydrous, 99.8%), acetone (Fisher Scientific, certified), tetrahydrofuran (THF, Sigma-Aldrich, PHT as inhibitor, 99.9%), N,N-dimethylformamide (DMF, Sigma-Aldrich, anhydrous, 99.8%), and N,N-dimethylacetamide (DMAc, Sigma-Aldrich, anhydrous, 99.8%), ethanol (Decon Laboratories, 200 Proof), hexane (Sigma-Aldrich, Chromasolv®, for HPLC, ≥ 95%), glacial acetic acid (Fisher Scientific, Certified ACS Plus), dimethylsulfoxide (DMSO, Sigma-Aldrich, anhydrous, 99.9+%), N-Methyl-2-pyrrolidone (NMP, Sigma-Aldrich, Chromasolv® Plus, for HPLC, ≥ 99%), pyridine (Sigma-Aldrich, anhydrous, 99.8%), chloroform (Fisher Scientific, HPLC grade, pentane stabilized), and dichloromethane (DCM, Fisher Scientific, stabilized, Certified ACS Plus). All reagents were used, as received, without any additional purification steps involved. Lacey carbon or holey carbon copper grids were obtained from (Ted Pella, Inc.) for TEM and SEM study.

Procedure

All co-solvents were mixed by volume unless otherwise noted. In a typical experiment, 5 mg of as-produced BNNT material was weighed out in a sample vial within a glove-box containing an electrostatic neutralizer to prevent static charge interference in order to reliably measure small amounts of BNNTs. Next, 20 mL of the desired solvent or co-solvent mixture was added to the sample vial for a final concentration of 0.25 mg/mL BNNT. The sample was magnetically stirred for 4 days (96 hours) to allow for sufficient interaction between the nanotubes and the solvent(s). Subsequently, the sample was placed in a 45 kHz, 80 W ultrasonic water bath (Fisher Scientific Ultrasonic Bath Model FS20H) and subjected to two sequential 15 minute segments to assess the dispersion state as a function of sonication time. The samples were checked again after settling for 1 day (24 hours) and 1 week (168 hours) post-sonication. An optical image of the dispersion was recorded immediately after each step to aid in assessing the dispersion state.

Characterization

Microscopy was conducted with a field emission Hitachi S-5200 high resolution scanning electron microscope (HR-SEM), with a through-the-lens detector, to capture high-contrast images of the dispersed material. A field emission JEOL JEM-2100F high-resolution transmission electron microscope (HRTEM) was also used to image the as-grown BNNTs. Dispersion samples were prepared by placing a drop of the supernatant onto a lacey carbon or holey carbon grid. The samples were then dried in air or in a vacuum oven, depending on the boiling point of the solvent/co-solvent utilized in the solution. To image the raw BNNTs, the nanotubes were not dispersed prior to TEM grid prep to observe any changes as a result of the dispersion process. In this case, the grid was pre-wet with ethanol and swiped across the container to collect the BNNTs for imaging.

The quality of the dispersion was assessed for selected single solvents and all co-solvents with UV-Vis spectroscopy after a settling time of 2 months at ambient temperature. The supernatants of each solution were pipetted into a quartz cuvette and analyzed with a Perkin Elmer Lambda 900 UV/Vis/NIR spectrometer. A cuvette filled with the pure solvent or co-solvent of interest was used as the reference cell. Liquid samples were analyzed over a range of 300 – 800 nm (350 nm for acetone and 325 for toluene) due to the UV-Vis cutoff of the organic solvents utilized in this work. In the case of raw BNNTs, UV-Vis data were collected on dried BNNTs on a quartz slide over the range of 190 – 800 nm. This was prepared by first stirring the as-synthesized material in acetone to break down the large pieces. The solution was subsequently transferred onto a quartz slide by pipette and dried to remove the solvent.

Optical absorption in the mid-infrared (mid-IR) region was measured for raw BNNTs using a Nexus 670 FT-IR (Thermo Nicolet) instrument equipped with a single-reflectance diamond attenuated total reflectance (ATR) accessory, with a KBr beam splitter in conjunction with a MCT/A detector. The data shown represent an average of 64 accumulated spectra over the range of 4000 – 650 cm^{-1}. Thermogravimetric analysis (TGA) was collected under air with a Seiko Instruments TG/DTA 220 from room temperature to 1000°C at a rate of 10°C/min.

Conclusions

In this work, single solvent studies were used to identify a region of good BNNT dispersion based on the thermodynamic Hansen parameters. Of the solvents tested, DMAc was found to disperse BNNTs at concentration of 0.25 mg/mL with mild sonication without destruction of the nanotube or shortening effects. The dispersion was found to remain stable without any sedimentation even after sitting for 1 week. BNNTs in DMF were comparable to DMAc, though noticeable sedimentation occurred over time. Both NMP and acetone also displayed long-term dispersion of BNNTs at a lower concentration than DMAc and DMF. Other solvents, namely THF, IPA, and MeOH, were effective at dispersing lower concentrations of BNNTs well over a shorter time period (up to 24 hours). Based on the good dispersion of BNNTs in DMAc, DMF, acetone, and NMP, a 3D solubility region was proposed around the central point of 16.8, 12.1, and 9.2 $MPa^{1/2}$ for δ_d, δ_p, and δ_h, respectively.

Utilizing the experimentally determined solubility parameters and proposed solubility region, a series of co-solvents were studied to improve the dispersion in poor solvents, namely toluene, ethanol, hexane, DCM, DMSO, and water. With the exception of water, it was demonstrated that by choosing a suitable co-solvent, BNNTs could be effectively dispersed in these solvents through this thermodynamic approach. Moreover, many of these dispersions were stable even after 2 months of settling time. Through the use of UV-Vis spectroscopy, both DMF-acetone and THF-NMP were found to exhibit more stable long-term dispersion of BNNTs than DMAc alone. These data were utilized to assess the solubility region

of BNNTs. With the incorporation of the good co-solvent systems, a refined solubility region was determined centered about 16.8, 10.7, and 9.0 $MPa^{1/2}$ for δ_d, δ_p, and δ_h, respectively. With all good solvents and co-solvents encompassed within the refined region, the Hansen solubility parameters for BNNTs are expected to lie close to the midpoint with a calculated Hildebrand parameter of 21.8 $MPa^{1/2}$.

It was demonstrated that improved BNNT dispersion can be realized with the use of a co-solvent system optimized to have solubility parameters within the solubility sphere of BNNT. Although the method is not perfect, as evidenced by some exceptions (THF-hexane and DMF-DCM), this approach was extremely versatile and it can be extended to other applications. For example, polymers, surfactants, and other molecules can be chosen from within this region as 'co-solvents' for BNNT dispersion. In addition, creating optimal co-solvent systems enables the utilization of a wider variety of solvents and polymers during nanocomposite fabrication for specific applications, cost effectiveness, and environmental awareness. This can greatly improve the fabrication processes of BNNT composites, thin films, coatings, and paintings. Alternatively, a suitable co-solvent can potentially be designed to effectively disperse BNNTs for a given molecule that lies outside of the solubility region.

Acknowledgements

This work was supported in part by the NASA Langley Creativity and Innovation, Internal Research and Development, and Bid and Proposal programs, as well as the NASA Game Changing Development Seedling programs. C. Park acknowledges funding in part by the US Air Force Office of Scientific Research - Low Density Materials program under Grant No. FA9550-11-1-0042. The authors also thank the Langley Aerospace Research Summer Scholars (LARSS) and the NASA Langley Research Center Undergraduate Research Program (USRP) for their sponsorship of R. Silva and M. Tsui. The authors would also like to thank Dr. Sang-Hyon Chu and Dr. Siviram Arepalli for fruitful discussions and helpful comments on this work. C. Park also thanks Dr. W. Cao for HRTEM imaging of BNNTs.

Notes and references

1. A. Rubio, J. L. Corkill and M. L. Cohen, *Phys. Rev. B*, 1994, **49**, 5081.
2. N. G. Chopra, R. J. Luyken, K. Cherrey, V. H. Crespi, M. L. Cohen, S. G. Louie and A. Zettl, *Science*, 1995, **269**, 966.
3. M. L. Cohen and A. Zettl, *Phys. Today*, 2010, **63**, 34.
4. X. Blase, A. Rubio, S. G. Louie and M. L. Cohen, *Europhys. Lett.*, 1994, **28**, 335.
5. N. G. Chopra and A. Zettl, *Solid State Commun.*, 1998, **105**, 297.
6. R. Arenal, M.-S. Wang, Z. Xu, A. Loiseau and D. Golberg, *Nanotechnology*, 2011, **22**, 265704.
7. X. Chen, L. Zhang, C. Park, C. C. Fay, X. Wang and C. Ke, *Appl. Phys. Lett.*, 2015, **107**, 253105.
8. Y. Chen, J. Zou, S. J. Campbell and G. Le Caer, *Appl. Phys. Lett.*, 2004, **84**, 2430.
9. Y. Xiao, X. H. Yan, J. X. Cao J. W. Ding, Y. L. Mao and J. Xiang, *Phys. Rev. B*, 2004, **69**, 205415
10. D. Golberg, Y. Bando, K. Kurashima and T. Sato, *Scr. Mater.*, 2001, **44**, 1561.
11. S. M. Nakhmanson, A. Calzolari, V. Meunier, J. Bernholc and M. Buongiorno Nardelli, *Phys. Rev. B*, 2003, **67**, 235406.
12. V. Yamakov, C. Park, J. H. Kang, K. E. Wise and C. C. Fay, *Comp. Mater. Sci.*, 2014, **95**, 362.
13. J. H. Kang, G. Sauti, C. Park, V. Yamakov, K. E. Wise, S. E. Lowther, C. C. Fay, S. A. Thibeault and R. G. Bryant, *ACS Nano*, 2015, **9**, 11942.
14. A. Tiano, C. Park, J. W. Lee, H. Luong, L. J. Gibbons, S.-H. Chu, S. I. Applin, P. Gnoffo, S. E. Lowther, H. J. Kim, P. M. Danehy, J. A. Inman, S. B. Jones, J. H. Kang, G. Sauti, V. Yamakov, K. E. Wise, J. Su and C. C. Fay, *Proc. SPIE*, 2014, **9060**, 906006.
15. S. A. Thibeault, J. H. Kang, G. Sauti, C. Park, C. C. Fay and G. C. King, *MRS Bull.*, 2015, **40**, 836.
16. Y. Chen, L. T. Chadderton, J. F. Gerald and J. S. Williams, *Appl. Phys. Lett.*, 1999, **74**, 2960.
17. A. Pakdel, C. Zhi, Y. Bando, T. Nakayama and D. Golberg, *Nanotechnology*, 2012, **23**, 215601.
18. A. Loiseau, F. Willaime, N. Demoncy, G. Hug and H. Pascard, *Phys. Rev. Lett.*, 1996, **76**, 4737.
19. R. Arenal, O. Stephan, J.-L. Cochon and A. Loiseau, *J. Am. Chem. Soc.*, 2007, **129**, 16183.
20. T. Laude, Y. Matsui, A. Marraud and B. Jouffrey, *Appl. Phys. Lett.*, 2000, **76**, 3239-3241.
21. J. Wang, V. K. Kayastha, Y. K. Yap, Z. Fan, J. G. Lu, Z. Pan, I. N. Ivanov, A. A. Puretzk and D. B. Geohegan, *Nano Lett.*, 2005, **5**, 2528.
22. M. W. Smith, K. C. Jordan, C. Park, J.-W. Kim, P. T. Lillehei, R. Crook and J. S. Harrison, *Nanotechnology*, 2009, **20**, 505604.
23. K. S. Kim, C. T. Kingston, A. Hrdina, M. B. Jakubinek, J. Guan, M. Plunkett and B. Simard, *ACS Nano*, 2014, **8**, 6211.
24. A. Fathalizadeh, T. Pham, W. Mickelson and A. Zettl, *Nano Lett.*, 2014, **14**, 4881.
25. J. N. Coleman, U. Khan, W. J. Blau and Y. K. Gun'ko, *Carbon*, 2006, **44**, 1624.
26. S. Mukhopadhyay, S. Gowtham, R. H. Scheicher, P. Ravindra and S. P. Karna, *Nanotechnology*, 2010, **21**, 165703.
27. K. Fu and Y.-P. Sun, *J. Nanosci. Nanotechnol.*, 2003, **3**, 351.
28. L. Hu, D. S. Hecht and G. Grüner, *Chem. Rev.*, 2010, **110**, 5790.
29. M. F. Islam, E. Rojas, D. M. Bergey, A. T. Johnson and A. G. Yodh, *Nano Lett.*, 2003, **3**, 269.
30. Z. Gao, C. Zhi, Y. Bando, D. Golberg and T. Serizawa, *J. Am. Chem. Soc.*, 2010, **132**, 4976.
31. Z. Gao, C. Zhi, Y. Bando, D. Golberg and T. Serizawa, *ACS Appl. Mater. Interfaces*, 2011, **3**, 627-632.
32. J. Yu, Y. Chen and B. M. Cheng, *Solid State Commun.*, 2009, **149**, 763.
33. C. H. Lee, D. Zhang and Y. K. Yap, *J. Phys. Chem. C*, 2011, **116**, 1798.
34. C. Zhi, Y. Bando, C. Tang, R. Xie, T. Sekiguchi and D. Golberg, *J. Am. Chem. Soc.*, 2005, **127**, 15996.
35. C. Zhi, Y. Bando, C. Tang, S. Honda, K. Sato, H. Kuwahara and D. Golberg, *Angew. Chem., Int. Ed.*, 2005, **44**, 7932.
36. M. Mutz, E. Eastwood and M. D. Dadmun, *J. Phys. Chem. C*, 2013, **117**, 13230.
37. S. D.; Bergin, V.; Nicolosi, P. V.; Streich, S.; Giordani, Z.; Sun, A. H.; Windle, P.; Ryan, N. P. P.; Niraj, Z.-T. T.; Wang, L., Carpenter, W. J. Blau, J. J. Boland, J. P. Hamilton and J. N. Coleman, *Adv. Mater.*, 2008, **20**, 1876.
38. J. M. Hughes, D. Aherne, S. D. Bergin, A. O'Neill, P. V. Streich, J. P. Hamilton and J. N. Coleman, *Nanotechnology*, 2012, **23**, 265604.
39. M.; Rubinstein and R. H. Colby, *Polymer Physics*. Oxford University Press: 2003.
40. C. M. Hansen, *Hansen Solubility Parameters: A User's Handbook, Second Edition*. Taylor & Francis: 2007.

41. J. M. G. Cowie, M. A. Mohsin and I. J. McEwen, *Polymer*, 1987, **28**, 1569.
42. S. D. Bergin, Z. Sun, D. Rickard, P. V. Streich, J. P. Hamilton and J. N. Coleman, *ACS Nano*, 2009, **3**, 2340.
43. Y. Hernandez, M. Lotya, D. Rickard, S. D. Bergin and J. N. Coleman, *Langmuir*, 2009, **26**, 3208.
44. G.-W. Lee and S. Kumar, *J. Phys. Chem. B*, 2005, **109**, 17128.
45. H. Chen, H. Muthuraman, P. Stokes, J. Zou, X. Liu, J. Wang, Q. Huo, S. I. Khondaker and L. Zhai, *Nanotechnology*, 2007, **18**, 415606.
46. H. T. Ham, Y. S. Choi and I. J. Chung, *J. Colloid Interface Sci.*, 2005, **286**, 216.
47. http://www.accudynetest.com/solubility_table.html
48. M. S. Strano, V. C. Moore, M. K. Miller, M. J. Allen, E. H. Haroz, C. Kittrell, R. H. Hauge and R. E. Smalley, *J. Nanosci. Nanotechnol.*, 2003, **3**, 81.
49. K. Yum and M.-F., Yu, *Nano Lett.*, 2006, **6**, 329.